RSC Advances

ROYAL SOCIETY
OF CHEMISTRY

www.rsc.org/advances

Table of contents entry

The Luminescence of Ion-exchangeable Defect Pyrochlore $KNbWO_6 \cdot H_2O:xEu^{3+}$

Yong Nam Han,[†] *Shihui Jiao, Man Xu, Yaohua Xu, Guangsheng Pang* and Shouhua Feng*

State Key Laboratory of Inorganic Synthesis and Preparative Chemistry, College of Chemistry,

Jilin University, Changchun 130012, P. R. China

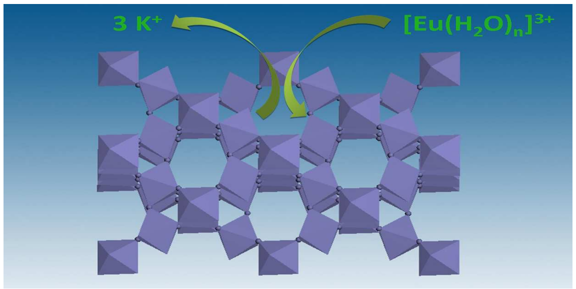

Defect pyrochlore structure with accessible channels serve as favorite host to incorporate Eu^{3+} ion.

Journal Name
RSCPublishing

ARTICLE

The Luminescence of Ion-exchangeable Defect Pyrochlore $KNbWO_6 \cdot H_2O$:xEu^{3+}

Cite this: DOI: 10.1039/x0xx00000x

Received 00th January 2012,
Accepted 00th January 2012

DOI: 10.1039/x0xx00000x

www.rsc.org/

Yong Nam Han, † Shihui Jiao, Man Xu, Yaohua Xu, Guangsheng Pang* and Shouhua Feng

$KNbWO_6 \cdot H_2O$:xEu^{3+} is prepared by ion exchange under hydrothermal conditions. Three K+ ions of $KNbWO_6 \cdot H_2O$ are exchanged by one Eu^{3+} ion and $KNbWO_6 \cdot H_2O$:xEu^{3+} keeps its defect pyrochlore structure. Thermal analysis results indicate that Eu^{3+} ion incorporates into the channels of defect pyrochlore structure in the form of aqueous ion $[Eu(H_2O)n]^{3+}$. $[Eu(H_2O)n]^{3+}$ in the channel losses water at 450 °C, which is much higher than that of $KNbWO_6 \cdot H_2O$. The hydration of Eu^{3+} ion in the pyrochlore structure has significant influence on the luminescence properties of $KNbWO6 \cdot H_2O$:xEu^{3+}. The emission intensity increases 10 times when the as-prepared $KNbWO_6 \cdot H_2O$:xEu^{3+} is annealed at 450 °C for 2 h.

Introduction

Phosphors with an inorganic host are ideal illuminating source due to their environmental friendliness, low energy consumption and adjustable colors.[1] Several inorganic compounds, such as YVO_4,[2] aluminates,[3] layered perovskite,[4] have been used as phosphor host. Pyrochlore oxides with a general chemical formula of $A_2B_2O_6O'$ are considered good phosphor host due to their high chemical and physical stability.[5,6] The ideal pyrochlore structure can be described as an ordered $2 \times 2 \times 2$ superstructure of the defect-fluorite structure.[7,8] There is corner-sharing network of BO_6 octahedra with large channels occupied by the A_2O' chains.[9] Pyrochlore oxides allow a wide variety of chemical substitutions at A and B sites.[5] Due to their interesting structures and properties, Pyrochlore oxides have a variety of technological applications including superconductors,[10,11] ionically conducting solid-oxide fuel-cell components,[12,13] nuclear fuels waste disposal,[14] magnetic materials,[15-17] thermoelectric materials,[18] electrode materials,[19] and water splitting photocatalysts.[20] In the case of luminescent materials, pyrochlore $(Y_{1-x}Eu_x)_2Sn_2O_7$ films have been prepared by sol-gel method and five predominant orange-red band emissions are observed.[21] Eu-doped $Gd_2Zr_2O_7$ and $Eu_2Zr_2O_7$ have been tested as luminescence sensing of temperature, the results show that these compounds can work up to at least 1200 °C.[22] Pyrochlore oxides have also been used as upconversion phosphores hosts, in which an intense green emission along with a red emission is observed under the excitation at 980 nm.[23]

The emission wavelengths of Eu^{3+} due to intra-configurational f-f transitions are determined primarily by their local environment in the host crystals.[24,25] At a site with inversion symmetry, Eu^{3+} exhibits dominantly magnetic-dipole $^5D_0$-$^7F_1$ transition with emission wavelengths around 590 nm. While at a site without inversion, Eu^{3+} exhibits hypersensitive forced electric-dipole $^5D_0$-$^7F_2$ transition with emission wavelengths of approximately 610-620 nm.[21] In pyrochlore oxides, Eu^{3+} (ionic radius 1.067 Å, CN8) is expected to occupy A-site which usually has site symmetry D_{3d} (inversion centre). Both of the electric-dipole and the magnetic-dipole transitions appear simultaneously in pyrochlore luminescent materials, and in most cases, one of which is much stronger.[21,22,24,25] Due to the convenient chemical substitutions at the A and B sites in pyrochlore oxides, it is expected that Eu^{3+} crystal site symmetry could be easily lowered by chemical substitution. In fact, recent research shows that the luminescence properties can be enhanced by simple compositional adjustments in the quaternary pyrochlore-type red phosphors.[25] The defect pyrochlore AB_2O_6 can be derived by removing half of the A-cation from the ideal pyrochlore structure. Recently, we prepared $KNbWO_6 \cdot H_2O$ via a two-step solvothermal process.[26] The defect pyrochlore $KNbWO_6 \cdot H_2O$ exhibits excellent performance in the removal of toxic Pb^{2+} by ion exchange. In this paper, we report the preparation of Eu^{3+} doped $KNbWO_6 \cdot H_2O$ by ion exchange and its luminescence property.

Experimental

The synthesis of $KNbWO_6 \cdot H_2O$ has been described in the reference.[26] In a typical procedure, 1.0 g Nb_2O_5 and 5.0 g KOH are mixed in 60 ml distilled water, the mixture is then transferred into a 100 ml autoclave and reacted at 180 °C for 2

d. After cooling down naturally, a clear colorless solution of $K_8Nb_6O_{19}$ is obtained after separating the insoluble residue by centrifuging.[27] Then 2.4 ml $K_8Nb_6O_{19}$ solution (0.0186 mol/L) is added into 20 ml of n-octanol, and H_2WO_4 is added with a molar ratio of Nb^{5+} : W^{6+} = 1 : 2.5. HCl is used to adjust the pH value to 7.2. Solvothermal treatment is undertaken in a 40 ml autoclave at 220 °C for 2 d. After cooling down to room temperature naturally, the products are centrifuged, washed with distilled water and dried under vacuum at 60 °C for 10 h.

$KNbWO_6 \cdot H_2O$:xEu^{3+} is prepared by ion exchange of 0.05 g $KNbWO_6 \cdot H_2O$ in 2.5 ml $Eu(NO_3)_3$ solution with different concentrations of 0.05, 0.1, 0.2, and 0.3 mol/L, respectively. The hydrothermal treatment is performed in a 40 ml autoclave at 180 °C for 2 days. The products are filtered and washed 4 times with distilled water, and dried under vacuum at 60 °C for 10 h. According to EDX and ICP results (Electronic Supplementary Information), the products obtained in $Eu(NO_3)_3$ solution of 0.05, 0.1, 0.2, and 0.3 mol/L are referred to as $KNbWO_6 \cdot H_2O$:0.120Eu^{3+}, $KNbWO_6 \cdot H_2O$:0.131Eu^{3+}, $KNbWO_6 \cdot H_2O$:0.149Eu^{3+}, and $KNbWO_6 \cdot H_2O$:0.178Eu^{3+}, respectively. In order to study how the water influence on the luminescence of the products. $KNbWO_6 \cdot H_2O$:0.131Eu^{3+} is heated at 450 °C for 2 h, and the heated product is referred to as $KNbWO_6 \cdot H_2O$:0.131Eu^{3+}-450.

The X-ray powder diffraction (XRD) patterns of the products are recorded with a Rigaku D/MAX 2500/PC X-ray diffractometer with graphite-filtered Cu-Kα radiation (λ=0.15418 nm) at 40 kV and 200 mA, and collected at 2θ angles of 10-70° with 0.02°/step. The lattice parameters were determined by a least squares refinement using JADE software with estimated standard deviation of 0.001 Å. The luminescence spectra of the samples are obtained at room temperature using Edinburgh FL920 spectrofluorimeter with a 450W xenon flash lamp as the exciting source. Thermo gravimetric analysis is carried out on a TGA Q500 under N_2 condition with a heating rate of 10 °C/min from 20 °C to 800 °C.

Results and Discussion

Figure 1 shows the XRD patterns of $KNbWO_6 \cdot H_2O$:xEu^{3+} (x=0, 0.120, 0.131, 0.149, 0.178). The XRD patterns of all of the samples can be well indexed into defect pyrochlore structure with a space group Fd-3m. No impurity has been found, and the marked peaks match well with JCPDS no. 25-0668 ($KNbWO_6 \cdot H_2O$). The calculated lattice parameter a=10.463 Å of $KNbWO_6 \cdot H_2O$:0.120Eu^{3+} decreased comparing with that of undoped $KNbWO_6 \cdot H_2O$ (a=10.499 Å). There is no significant difference in lattice parameter for sample $KNbWO_6 \cdot H_2O$:0.131Eu^{3+}, $KNbWO_6 \cdot H_2O$:0.149Eu^{3+} and $KNbWO_6 \cdot H_2O$:0.178Eu^{3+}. Figure 1f shows the XRD pattern of $KNbWO_6 \cdot H_2O$:0.131Eu^{3+}-450, which indicates that the sample keeps defect pyrochlore structure after annealing at 450 °C.

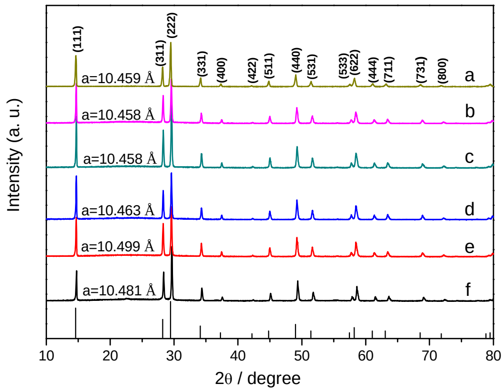

Figure 1 XRD patterns of $KNbWO_6 \cdot H_2O$:xEu^{3+}, (a) x=0.178, (b) x=0.149, (c) x=0.131, (d) x=0.120, (e) x=0, and (f) $KNbWO_6 \cdot H_2O$:0.131Eu^{3+} annealed at 450 °C. The lattice parameters were determined by a least squares refinement using JADE software with estimated standard deviation of 0.001 Å.

Figure 2 shows the TG curves of $KNbWO_6 \cdot H_2O$, $KNbWO_6 \cdot H_2O$:0.131Eu^{3+}, and $KNbWO_6 \cdot H_2O$:0.131$Eu3^{+}$-450. The weight losses are 3.64 % for $KNbWO_6 \cdot H_2O$ (Figure 2b), 6.07% for $KNbWO_6 \cdot H_2O$:0.131Eu^{3+} (Figure 2c), and 3.30 % for $KNbWO_6 \cdot H_2O$:0.131Eu^{3+}-450 (Figure 2a), respectively. The theoretical weight loss for $KNbWO_6 \cdot H_2O$:0.131Eu^{3+} is 4.05 %. The deviation from the ideal weight loss value is attributed to more water being trapped in the channel than expected. While $KNbWO_6 \cdot H_2O$ is treated in $Eu(NO_3)_3$ solution under hydrothermal condition, to keep the charge balance, three K^+ ions (ionic radius 0.133 nm) are expected to be exchanged by one Eu^{3+} ion (ionic radius 0.1067 nm, CN8), as a result two K^+ vacancies accompany one Eu^{3+} ion. Both of the smaller ionic radius and less occupancy of the original K^+ position in the defect pyrochlore structure are responsible for the decrease in lattice parameter. It is understandable that more water molecules will move into the channels of the crystal to occupy the space left by K^+ ions. The higher weight loss temperature also implies the possibility that the additional water exist as aqueous ion $[Eu(H_2O)_n]^{3+}$. The less changable lattice parameter with Eu^{3+} doping of $KNbWO_6 \cdot H_2O$ is possible due to the influence of aqueous ion. The experimentally determined weight loss shows that $KNbWO_6 \cdot H_2O$:0.131Eu^{3+}-450 has partial hydration at room temperature (Figure 2a). Defect pyrochlores are known to absorb moisture and $KNbWO_6$ is easily hydrated in air at room temperature. Therefore, the additional weight lost by $KNbWO_6 \cdot H_2O$:0.131Eu-450 is not surprising.

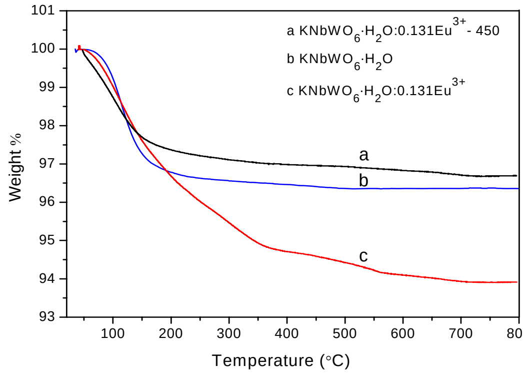

Figure 2 TG curves of (a) $KNbWO_6{\cdot}H_2O$:0.131Eu^{3+} annealed at 450 °C, (b) $KNbWO_6{\cdot}H_2O$, and (c) $KNbWO_6{\cdot}H_2O$:0.131Eu^{3+}.

Figure 3a shows the excitation and emission spectra of $KNbWO_6{\cdot}H_2O$:xEu^{3+} (x=0.120, 0.131, 0.149, 0.178). The excitation spectra monitored at 610 nm have two strong excitation peaks at 394 nm and 464 nm, which are correspondence to $^7F_0$-$^5L_6$ and $^7F_0$-$^5D_2$ transitions, respectively.[24,24,28,29] Comparing to the excitation spectra of Eu:Lu_2O_3,[30] or pyrochlore $CaLaSnNbO_7$:Eu,[24] there is no charge transfer absorption band observed in the excitation spectra, which indicates that the interaction of Eu^{3+} ions and the host of $KNbWO_6{\cdot}H_2O$ is weaker than that in the case of Eu^{3+} ions in Lu_2O_3 or $CaLaSnNbO_7$. This is consistent with the fact that $KNbWO_6{\cdot}H_2O$:xEu^{3+} is prepared by ion exchange and Eu^{3+} ions are moveable in the structure of $KNbWO_6{\cdot}H_2O$.

All of the samples exhibit similar emission spectra with excitation wavelength of 464 nm. As shown in Figure 3b, there is one peak at 580 nm which is referred to $^5D_0$-$^7F_0$ transition, three peaks between 584 and 604 nm which are attributed to $^5D_0$-$^7F_1$ transition, five peaks between 604 and 670 nm can ascribed to $^5D_0$-$^7F_2$ transition. This result is in good agreement with that of the literatures.[25,31,32] The clear sharp peak at 580 nm suggesting that Eu^{3+} ions are located in a site with lower symmetry. $^5D_0$-$^7F_0$ transition is an electronic transition between nondegenerate levels and has an electric dipole character. This transition is formally forbidden when the free-ion is considered but is allowed in the solid under certain conditions.[32] It is known that $^5D_0$-$^7F_1$ transition is driven by the magnetic dipole and the intensity is supposed to be practically independent from the crystal field. In contrast, the intensity of $^5D_0$-$^7F_1$ transitions is smaller than that of $^5D_0$-$^7F_2$ transitions in Figure 3b, and the ratio of these intensities (I $^5D_0$-$^7F_1$/I $^5D_0$-$^7F_2$) is less than unity indicating that Eu^{3+} ions in $KNbWO_6{\cdot}H_2O$:xEu^{3+} locate inhomogeneously at the sites without inversion symmetry.[25]

The relative luminescence intensity depends on the x value, the luminescence intensity of $KNbWO_6{\cdot}H_2O$:0.131Eu^{3+} increase quickly compared to that of $KNbWO_6{\cdot}H_2O$:0.120Eu^{3+}, and then decrease for higher x value due to a concentration quenching effecting. $KNbWO_6{\cdot}H_2O$:0.131Eu^{3+} is the best doping concentration of Eu^{3+} for the high performance of luminescence property. More Eu^{3+} doping will decrease the luminescence of the phosphors. It is known that when the Eu^{3+} concentration increases, the rate of exchange energy transfer increases, which leads to the trapping of excitation energy by some killer sites and leads to increased nonradiative transition rates and hence quenching in luminescence.[25]

Water molecules can effectively quench the luminescence of $KNbWO_6{\cdot}H_2O$:xEu^{3+}, which is confirmed by comparing the luminescence of the samples with and without water of $[Eu(H_2O)_n]^{3+}$. Figure 4 shows the excitation spectra (em=610 nm) and emission spectra (ex=464 nm) spectra of $KNbWO_6{\cdot}H_2O$:0.131Eu^{3+} and $KNbWO_6{\cdot}H_2O$:0.131Eu^{3+}-450. As shown in Figure 4a, the intensities of excitation peaks at 394 and 464 nm are almost the same for $KNbWO_6{\cdot}H_2O$:0.131Eu^{3+}. After heated at 450 °C, the intensity of excitation peak at 464 nm becomes almost 12 times of that at 394 nm. Similar behavior is observed in the emission spectra (Figure 4b), the emission ascribed to the $^5D_0$-$^7F_2$ transition increased 10 times after calcination. This result indicates that the water of $[Eu(H_2O)_n]^{3+}$ in the channels strongly influence the luminescence. The nonradiative transition caused by hydration may be the possible reason for luminescence quenching. There are also reports that water molecules are the main factor leading to the quenching in luminescence for $Eu_2Mo_7O_{24}{\cdot}4H_2O$ and $Eu_8(WO_7)_3{\cdot}5H_2O$.[33]

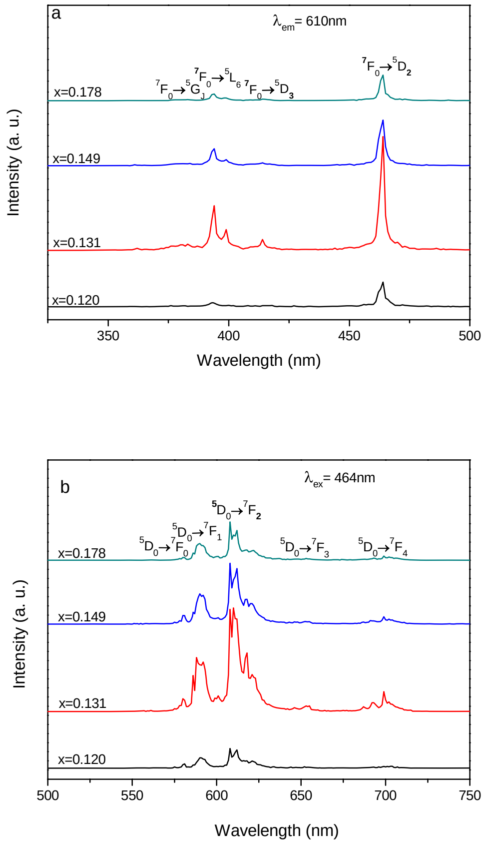

Figure 3 Exciation (a) and emission spectra (b) of $KNbWO_6{\cdot}H_2O$:xEu^{3+} (x= 0.120, 0.131, 0.149, 0.178).

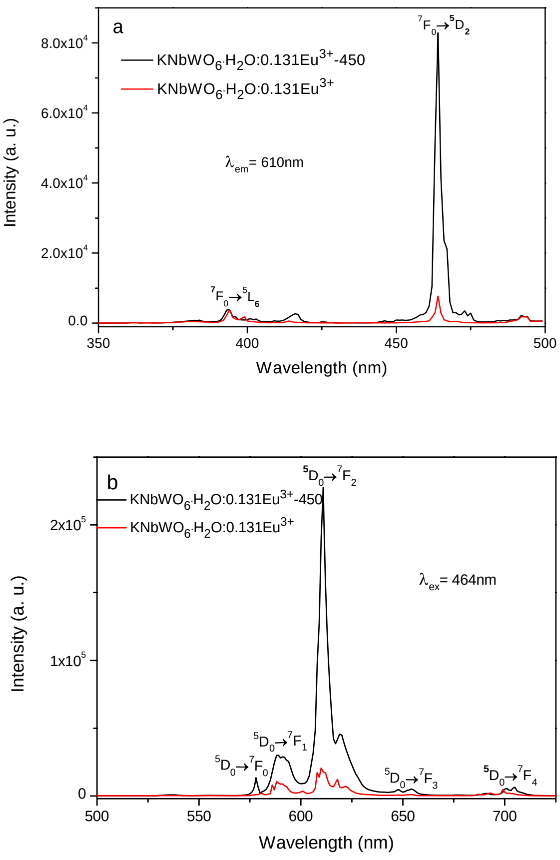

Figure 4 Excitation (a) and emission spectra (b) of KNbWO$_6$·H$_2$O:0.131Eu^{3+} and KNbWO$_6$·H$_2$O:0.131Eu^{3+} annealed at 450°C.

Figure 5 shows the decay curves of Eu^{3+} emission resulting from $^5D_0$-$^7F_2$ under excitation at 464 nm. The as-prepared KNbWO$_6$·H$_2$O:xEu^{3+} with x= 0.120, 0.131, 0.149, and 0.178 have similar photoluminescence decay curves. Whereas a significant increase of lifetime is observed for KNbWO$_6$·H$_2$O:0.131Eu^{3+}-450. The decay curves can be fitted suing a single exponential decay function,

$$y = A\exp(-t/T) + y_0$$

where y is the photoluminescence intensity, t is the time, y_0 and A are constants and T is the emission lifetime. The observed lifetime of the as-prepared KNbWO$_6$·H$_2$O:xEu^{3+} with x= 0.120, 0.131, 0.149, and 0.178 are 0.246, 0.292, 0.262, and 0.257 ms, respectively. The lifetime of KNbWO$_6$·H$_2$O:0.131Eu^{3+}-450 increase to 0.475 ms. The Quantum efficiency of KNbWO$_6$·H$_2$O:0.131Eu^{3+} annealed at 450 °C is estimated to be 21.9 %.

Figure 6 shows the structure of KNbWO$_6$·H$_2$O along [1 1 0] direction. There are one-dimensional interconnected channels formed by corner-shared MO$_6$ octahedra. K$^+$ and H$_2$O occupy alternately along the channels. While KNbWO$_6$·H$_2$O is treated in Eu(NO$_3$)$_3$ solution under hydrothermal condition, three K$^+$ ions are exchanged by one Eu^{3+} ion. There are two K$^+$ vacancies accompany one Eu^{3+} ion, which result that Eu^{3+} ion get into the channels as aqueous ion [Eu(H$_2$O)$_n$]$^{3+}$. The as-prepared KNbWO$_6$·H$_2$O:xEu^{3+} shows poor luminescence due to quenching effect of water. While as-prepared KNbWO$_6$·H$_2$O:xEu^{3+} is annealed at 450 °C, The aqueous ion [Eu(H$_2$O)$_n$]$^{3+}$ losses water irreversible. The dehydration of KNbWO$_6$·H$_2$O:xEu^{3+} is also reflected by the luminescence properties. The local environment around Eu^{3+} has influence on the electric-dipole $^5D_0$-$^7F_2$ transition.[28,29] An intense red emission band at 612 nm of KNbWO$_6$·H$_2$O:0.131Eu^{3+}-450 imply that the Eu^{3+} locate at a less symmetry environment comparing to that of the as-prepared KNbWO$_6$·H$_2$O:0.131Eu^{3+}.

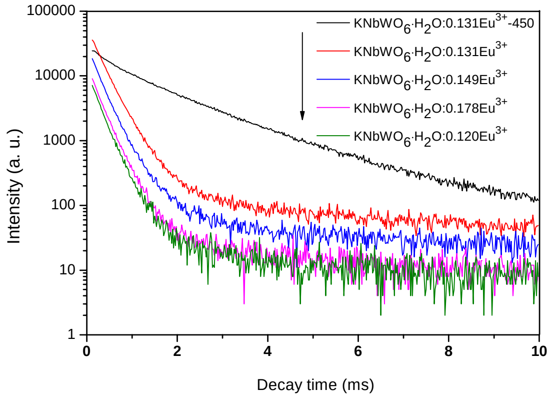

Figure 5 The decay curves of Eu^{3+} emission resulting from $^5D_0$-$^7F_2$ under excitation at 464 nm for the as-prepared KNbWO$_6$·H$_2$O:xEu^{3+} with x= 0.120, 0.131, 0.149, 0.178 and KNbWO$_6$· H$_2$O:0.131Eu^{3+}-450.

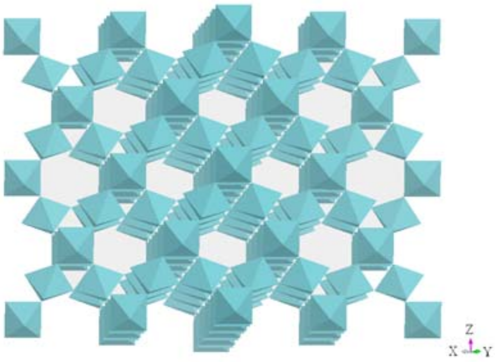

Figure 6 the structure of KNbWO$_6$·H$_2$O along [1 1 0] direction.

Conclusions

KNbWO$_6$·H$_2$O is an ideal ion exchange material for trivalent metal ions. Three K$^+$ ions of KNbWO$_6$·H$_2$O are exchanged by one Eu^{3+} ion under hydrothermal conditions. The amount of doping Eu^{3+} ion in defect pyrochlore structure can be adjusted by changing the hydrothermal conditions. Thermal analysis results indicate that Eu^{3+} ion get into the channel of defect pyrochlore structure in the form of aqueous ion [Eu(H$_2$O)$_n$]$^{3+}$. The water of [Eu(H$_2$O)$_n$]$^{3+}$ loss at temperature of 450 °C, which is much higher than that of $KNbWO_6\cdot H_2O$. The hydration of Eu^{3+} ion in the pyrochlore structure has significant influence on the luminescence property of $KNbWO_6\cdot H_2O:xEu^{3+}$. 10 times increase of the emission intensity is observed for the as-prepared $KNbWO_6\cdot H_2O:xEu^{3+}$ annealed at 450 °C for 2 h. The $KNbWO_6\cdot H_2O$ with defect pyrochlore structure can be used as efficient luminescent host.

Acknowledgements

This work is supported by the National Natural Science Foundation of China (no. 21071058, 21371066).

Notes and references

State Key Laboratory of Inorganic Synthesis and Preparative Chemistry, College of Chemistry, Jilin University, Changchun 130012, P. R. China
E-mail: panggs@jlu.edu.cn
[†]Permanent Address: Department of Chemistry, Kim Il Sung University, Pyongyang, Democratic People's Republic of Korea

Electronic Supplementary Information (ESI) available: [EDX and ICP results of $KNbWO_6\cdot H_2O:xEu^{3+}$ with x = 0.120, 0.131, 0.149, and 0.178.]. See DOI: 10.1039/b000000x/

1. C. Feldmann, T. Justel, C. R. Ronda and P. J. Schmidt, *Adv. Funct. Mater.*, 2003, **13**, 511-516.
2. Y. B. Liao, N. Chen and G. P. Du, *J. Alloys Compd.*, 2013, **561**, 214-219.
3. C. K. Chang, Z. X. Yuan and D. L. Mao, *J. Alloys Compd.*, 2006, **415**, 220-224.
4. A. Kudo, *Chem. Mater.*, 1997, **9**, 664-669.
5. A. El Haimouti, D. Zambon, M. El-Ghozzi, D. Avignant, F. Leroux, M. Daoud and M. El Aatmani, *J. Alloys Compd.*, 2004, **363**, 130-137.
6. K. Holliday, S. Finkeldei, S. Neumeier, C. Walther, D. Bosbach and T. Stumpf, *J. Nucl. Mater.*, 2013, **433**, 479-485.
7. Y. Liu, R. L. Withers and L. Norén, *J. Solid State Chem.*, 2004, **177**, 4404-4412.
8. C. Karthik, T. J. Anderson, D. Gout and R. Ubic, *J. Solid State Chem.*, 2012, **194**, 168-172.
9. G. D. Blundred, G. A. Bridges and M. J. Rosseinsky, *Angew. Chem. Int. Ed.*, 2004, **43**, 3562-3565.
10. J. Yamaura, S. Yonezawa, Y. Muraoka and Z. Hiroi, *J. Solid State Chem.*, 2006, **179**, 336-340.
11. M. Hanawa, J. Yamaura, Y. Muraoka, F. Sakai and Z. Hiroi, *J. Phys. Chem. Solids*, 2002, **63**, 1027-1030.
12. M. E. Björketun, C. S. Knee, B. J. Nyman and G. Wahnström, *Solid State Ionics*, 2008, **178**, 1642-1647.
13. W. R. Panero, L. Stixrude and R. C. Ewing, *Phys. Rev. B*, 2004, **70**, 054110.
14. G. R. Lumpkin, M. Pruneda, S. Rios, K. L. Smith, K. Trachenko, K. R. Whittle and N. J. Zaluzec, *J. Solid State Chem.*, 2007, **180**, 1512-1518.
15. K. Ramesha, L. Sebastian, B. Eichhorn and J. Gopalakrishnan, *J. Mater. Chem.*, 2003, **13**, 2011-2014.
16. G. T. Knoke, A. Niazi, J. M. Hill and D. C. Johnston, *Phys. Rev. B*, 2007, **76**, 054439.
17. X. G.Zheng, M. Hagihala, T. Kawae and C. N. Xu, *Phys. Rev. B*, 2008, **77**, 024418.
18. H. Y. Sang and J. F. Li, *J. Alloys Compd.* 2010, **493**, 678-682.
19. R. E. Carbonio, J. A. Alonso and J. L. Martinez, *J. Phys.: Condens. Matter.*, 1999, **11**, 361-369.
20. S. Ikeda, T. Itani, K. Nango and M. Matsumura, *Catal. Lett.*, 2004, **98**, 229-233.
21. S. Fujihara and K. Tokumo, *Chem. Mater.*, 2005, **17**, 5587-5593.
22. M. M. Gentleman and D. R. Clarke, *Surf. Coat. Technol.*, 2005, **200**, 1264-1269.
23. X. S. Li, H. T. Cai, L. H. Ding, X. W. Dou and W. F. Zhang, *J. Alloys Compd.*, 2012, **541**, 36-40.
24. S. K. Mahesh, P. P. Rao, M. Thomas, A. N. Radhakrishnan and P. Koshy, *J. Mater. Sci: Mater. Electron.*, 2012, **23**, 1605-1609.
25. S. K. Mahesh, P. P. Rao, M. Thomas, T. L. Francis and P. Koshy, *Inorg. Chem.*, 2013, **52**, 13304-13313.
26. Y. N. Han, S. H. Jiao, M. Xu G. S. Pang and S. H. Feng, *RSC Adv.*, 2014, **4 (28)**, 14357-14360.
27. Y. W. Zhang, C. Liu, G. S. Pang, S. H. Jiao, S. Y. Zhu, D. Wang, D. X. Liang and S. H. Feng, *Eur. J. Inorg. Chem.*, 2010, **8**, 1275-1282.
28. G. J. Gao, S. Reibstein, M. Y. Peng and L. Wondraczek, *J. Mater. Chem.*, 2011, **21**, 3156-3161.
29. G. J. Gao and L. Wondraczek, *J. Mater. Chem. C*, 2014, **2**, 691-695.
30. C. Martinet, A. Pillonnet, J. Lancok and C. Garapon, *J. Lumin.*, 2007, **126**, 807-816.
31. J. Lancok, C. Garapon, C. Martinet, J. Mugnier and R. Brenier, *Appl. Phys. A*, 2004, **79**, 1263-1265.
32. D. Machon, V. P. Dmitriev, V. V. Sinitsyn and G. Lucazeau, *Phys. Rev. B.*, 2004, **70**, 094117.
33. R. F. de Farias, C. Airoldi, M. F. Belian and S. Alvres, Jr., *J. Alloys Compd.*, 2006, **419**, 50-53.